The Astrophysical Journal Letters, 716:L14–L18, 2010 June 10 doi:10.1088/2041-8205/716/1/L14

IC 3418: STAR FORMATION IN A TURBULENT WAKE

Janice A. Hester[1], Mark Seibert[2], James D. Neill[1], Ted K. Wyder[1], Armando Gil de Paz[3], Barry F. Madore[2], D. Christopher Martin[1], David Schiminovich[4], and R. Michael Rich[5]
[1] California Institute of Technology, Pasadena, CA 91125, USA; jhester@srl.caltech.edu
[2] Observatories of the Carnegie Institute of Washington, Pasadena, CA 91101, USA
[3] Dpto. de Astrofísica, Universidad Computense de Madrid, Madrid 28040, Spain
[4] Department of Astronomy, Columbia University, New York, NY 10027, USA
[5] Department of Physics and Astronomy, Division of Astronomy and Astrophysics, University of California, Los Angeles, CA 90095, USA
Received 2010 February 22; accepted 2010 May 6; published 2010 May 19

ABSTRACT

Galaxy Evolution Explorer observations of IC 3418, a low surface brightness galaxy in the Virgo Cluster, revealed a striking 17 kpc UV tail of bright knots and diffuse emission. Hα imaging confirms that star formation is ongoing in the tail. IC 3418 was likely recently ram pressure stripped on its first pass through Virgo. We suggest that star formation is occurring in molecular clouds that formed in IC 3418's turbulent stripped wake. Tides and ram pressure stripping (RPS) of molecular clouds are both disfavored as tail formation mechanisms. The tail is similar to the few other observed star-forming tails, all of which likely formed during RPS. The tails' morphologies reflect the forces present during their formation and can be used to test for dynamical coupling between molecular and diffuse gas, thereby probing the origin of the star-forming molecular gas.

Key words: galaxies: clusters: individual (Virgo) – galaxies: individual (IC 3418) – ultraviolet: galaxies

1. INTRODUCTION

IC 3418, a faint low surface brightness galaxy ($M_r = -16.6$) in the Virgo Cluster, was observed with the *Galaxy Evolution Explorer* (*GALEX*; Martin et al. 2005) and was found to have a remarkable ultraviolet tail of bright knots and diffuse emission (Figure 1). The presence of near-ultraviolet (NUV), far-ultraviolet (FUV), and Hα (Gavazzi et al. 2006) in the knots indicates that star formation is ongoing. Galaxies with similar star-forming tails have been observed in other clusters at multiple wavelengths (Cortese et al. 2007; Yoshida et al. 2008; Sun et al. 2006, 2007). The UV morphology revealed in the moderately deep *GALEX* images of IC 3418 is a potentially powerful probe of its tail's formation mechanism.

It has been suggested that similar tails are either star formation in ram pressure (RP) stripped molecular clouds (Yoshida et al. 2008; Kronberger et al. 2008; Kapferer et al. 2009; Chung et al. 2009) or a combination of cloud stripping and gravitational interactions (Cortese et al. 2007, C07). None of these tails appears like known tidal features, and they consist preferentially of gas and young stars. We estimate that the tidal radii of all of these systems are beyond the disks' stellar radii.

Star formation occurs in simulated RP stripped wakes when cold clouds and diffuse H I are tightly dynamically coupled (Kronberger et al. 2008; Kapferer et al. 2009). Assuming strong dynamical coupling between the gas phases is likely invalid during ram pressure stripping (RPS). In simulations that resolve the multiphase medium, high-density clouds are not stripped (Tonnesen & Bryan 2009). For an observed example, isolated star-forming clouds remain in the disk of NGC 4402, another Virgo spiral, despite stripping of the H I (Crowl et al. 2005).

We suggest that the tail of IC 3418 represents in situ molecular cloud and star formation in the galaxy's turbulent wake following RPS. In Sections 2 and 3, we discuss the observations of IC 3418 and its star-forming tail. In Section 4, we show that while RPS of the H I is expected, theory disfavors removing H_2 from the galaxy via either stripping or tides. In Section 5, we discuss the morphologies of IC 3418 and similar star-forming tails; demonstrating that they favor in situ molecular cloud formation.

IC 3418 is beginning the transition between the blue and red sequences (NUV $- r = 2.75$) and is thus interesting in its own right. The stars in the tail may eventually contribute to the intracluster light (ICL), warranting a study of the frequency of these tails. We limit our study to the tail's formation.

2. IC 3418

GALEX observed IC 3418 in the FUV (1350–1750 Å) and the NUV (1750–2750 Å) between 2004 March and 2006 May with effective exposure times of 2 ks and 15 ks, respectively. An 1800 s Hα observation was taken on the ESO 3.6 m in 2005 and is publicly available (Gavazzi et al. 2003, 2006). The galaxy was observed by the Sloan Digital Sky Survey (SDSS; York et al. 2000), but optical colors cannot be measured for the tail. We adopt a distance to Virgo of 16.5 Mpc (Mei et al 2007), at which distance *GALEX*'s resolution is 400 pc (5″).

IC 3418 is a member of the Virgo Cluster at a projected distance of 450 kpc (94′) from the cluster's core with a recessional velocity of 38 km s^{-1} (Gavazzi et al. 2004). Virgo is a dynamically young cluster, as evidenced by substructure in the galaxy distribution and the X-ray emission (Binggeli et al. 1987; Schindler et al. 1999). Galaxies with H I tails which are presumably undergoing RPS are observed in Virgo's outskirts (Chung et al. 2007).

IC 3418's disk has blue optical colors but red UV colors relative to its optical colors and no Hα, suggesting that star formation was truncated on order 100 Myr ago (Figure 2). The disk appears truncated in the FUV relative to the NUV (Figure 1) and shows UV and optical color gradients (Figure 3) consistent with star formation having ceased first in the outer disk. Though irregular, the disk shows no signs of tidal disturbance (no structured streams or arms of disk stars). IC 3418 is not detected in H I ($M_{\rm H\,I} < 10^{6.9}\,M_\odot$), though a diffuse component in the tail has not been excluded (Chung et al. 2009). If IC 3418 is on its first orbit through Virgo, as many cluster members appear to be, it was likely accreted on order 100 Myr ago; 500 Myr

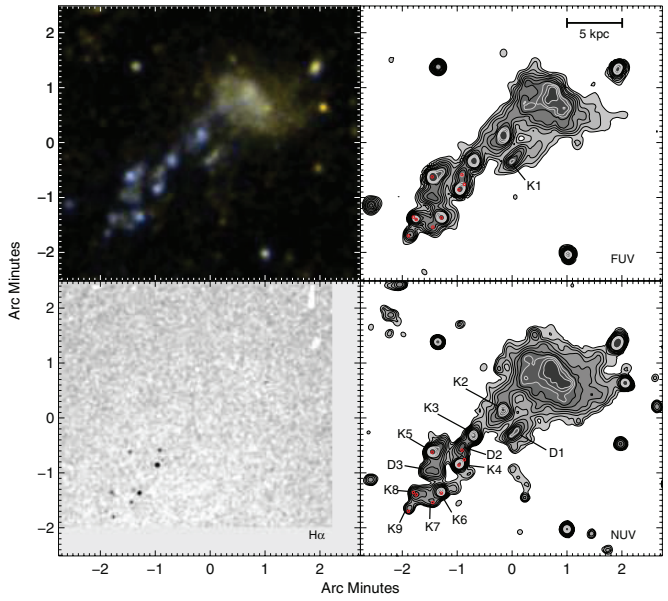

Figure 1. Imaging showing a 17 kpc tail of star formation trailing IC 3418 as it plunges through Virgo's ICM. Upper left: color composite ultraviolet image; FUV is blue, NUV is red, and the average UV intensity is green. Adaptive smoothing was performed using *asmooth* from the *XMM-Newton* Science Analysis Software package (http://xmm.esac.esa.int/sas). Upper right: FUV surface brightness. Contours are logarithmically spaced from 15e–17 to 200e–17 erg s^{-1} cm^{-2} arcsec^{2}. Red circles indicate Hα detections. The single knot defined in the FUV is labeled. Lower right: NUV surface brightness. Knots and diffuse regions discussed in the text are labeled. Lower left: Gavazzi et al. (2006) continuum-subtracted Hα image smoothed with an FWHM Gaussian of 0.″6.

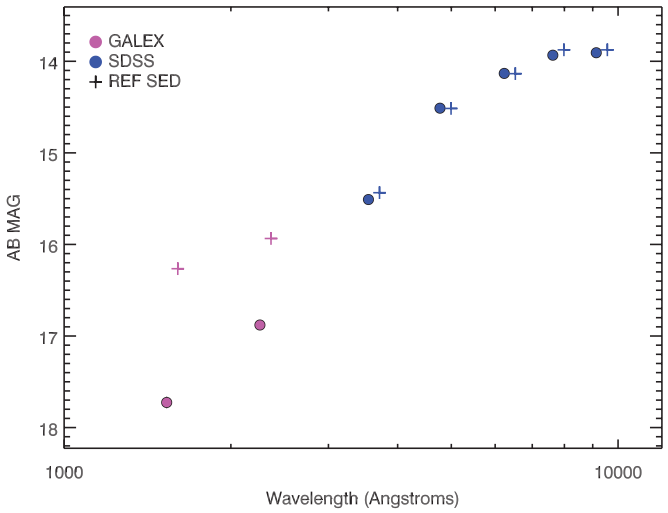

Figure 2. UV (*GALEX*) to optical (SDSS) SED of IC 3418's disk, measured within an elliptical aperture with a semimajor axis of 1.′2, an axis ratio of 0.68, and a position angle of 67.8. Emission from the knots and foreground stars was masked. The reference SED represents the average of ∼100 *GALEX*+SDSS galaxies with $-16.1 > M_r > -17.1$ and $0.3 < g - r < 0.45$.

being a generic cluster infall time. Together, these observations suggest IC 3418 was recently RP stripped by Virgo's intracluster medium (ICM).

3. STAR-FORMING TAIL

We visually separate the tail into bright circular knots and diffuse, asymmetric, lower surface brightness regions. The resolution of *GALEX* limits our interpretation of these objects. To measure luminosities, regions are defined using the outermost

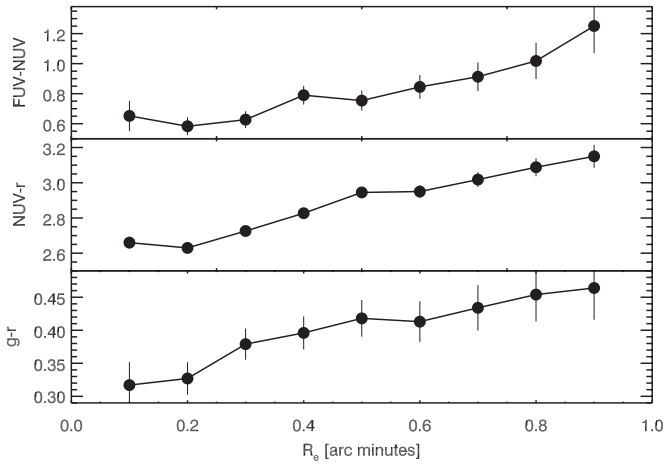

Figure 3. *GALEX*+SDSS color profiles of IC 3418's disk using 6″ annuli; masked as in Figure 2.

closed NUV surface brightness contour around each object, which are labeled in Figure 1. A discrete set of contours was considered, but given their dense spacing on the sky this should not impact our results.

The bright knots have NUV luminosities (νf_ν) between $1.3 \times 10^5\ L_\odot$ and $3.4 \times 10^6\ L_\odot$. The diffuse regions are redder in FUV–NUV than the knots; the average colors are 0.35 ± 0.06 and -0.02 ± 0.03, respectively (Table 1). The knots' colors are consistent with ongoing star formation. The total FUV luminosity of the tail, $3.3 \times 10^7\ L_\odot$, corresponds to a star formation rate (SFR) of $6 \times 10^{-3}\ M_\odot\ \mathrm{yr}^{-1}$ if star formation is ongoing (Salim et al. 2007). This is a lower limit; the knots may contain dust. A knot is also defined (k1) using the innermost FUV contour within the streamer at the tail's base (d1). Its FUV–NUV color is -0.08 ± 0.12, typical of the knots. Hα is found in the majority of the knots, indicating that star formation is ongoing. Hα is not observed in the three UV knots closest to IC 3418. They may be detected in deeper Hα imaging if they have a top-light initial mass function, could be a signature of the tail's formation mechanism, or could indicate RPS of gas from the stellar knots themselves. Only one Hα region is observed away from a UV peak.

4. ENVIRONMENT OF IC 3418

Within a cluster, tidal interactions and the ICM wind can strip mass from a galaxy's disk. We estimate the effects of both on IC 3418, noting that the lack of an appropriate neighbor excludes galaxy–galaxy tidal interactions. The H I in IC 3418's disk was extremely susceptible to RPS, as expected for a faint, low surface brightness galaxy orbiting in a massive cluster. In contrast, IC 3418's probable tidal radius is beyond its stellar disk, ruling out a tidal origin for the tail. The dense molecular clouds were unlikely to be RP stripped as clouds.

We first estimate the impact of RPS using the stripping condition of Gunn & Gott (1972),

$$\rho_{\mathrm{ICM}} v_{\mathrm{orbital}}^2 > 2\pi G \sigma_* \sigma_{\mathrm{H}}. \quad (1)$$

We use the usual β profile for the ICM density and adopt values of the profile slope, β, and the central density, ρ_0, for Virgo from Sanderson et al. (2003). Assuming a three-dimensional distance from the cluster's core of $\sqrt{2} r_{\mathrm{projected}}$ and an orbital velocity of $v_{\mathrm{orbital}} = 1000\ \mathrm{km\ s^{-1}}$, the ram pressure is $P_{\mathrm{ram}} = \rho_{\mathrm{ICM}} v_{\mathrm{orbital}}^2 \approx 40\ M_\odot\ \mathrm{pc^{-3}\ km^2\ s^{-2}}$.

Table 1
Properties of the Knots and Diffuse Regions (see Section 3 and Figure 1)

Name	R.A.	Decl.	Dist (′)	Dist (kpc)	FUV	NUV	FUV–NUV	Hα
IC 3418	12:29:43.82	11:24:09.30	...	...	17.73 ± 0.06	16.88 ± 0.03	0.85 ± 0.07	N
k1*	12:29:46.88	11:23:04.86	1.32	6.3	21.75 ± 0.12	21.83 ± 0.03	−0.08 ± 0.12	N
k2	12:29:47.59	11:23:33.36	1.12	5.4	20.36 ± 0.06	20.35 ± 0.02	0.01 ± 0.07	N
k3	12:29:49.84	11:23:06.36	1.84	8.8	20.74 ± 0.08	20.81 ± 0.02	−0.07 ± 0.08	N
k4	12:29:50.75	11:22:36.35	2.33	11.2	20.88 ± 0.08	20.82 ± 0.02	0.06 ± 0.08	Y
k5	12:29:52.59	11:22:49.85	2.56	12.3	20.12 ± 0.06	20.15 ± 0.01	−0.02 ± 0.06	Y
k6	12:29:52.29	11:22:04.86	2.96	14.2	20.76 ± 0.08	20.78 ± 0.02	−0.01 ± 0.08	Y
k7	12:29:52.90	11:21:54.35	3.20	15.3	23.4 ± 0.3	23.71 ± 0.08	−0.3 ± 0.3	Y
k8	12:29:53.92	11:22:01.85	3.30	15.8	21.5 ± 0.1	21.48 ± 0.03	−0.0 ± 0.1	Y
k9	12:29:54.53	11:21:46.85	3.58	17.2	23.1 ± 0.2	23.10 ± 0.06	−0.0 ± 0.2	Y
k1 ··· k9	...	...	...	...	18.60 ± 0.03	18.621 ± 0.007	−0.02 ± 0.03	...
d1*	12:29:46.57	11:23:10.86	1.19	5.7	20.84 ± 0.09	20.43 ± 0.02	0.41 ± 0.09	N
d2	12:29:50.65	11:22:52.85	2.13	10.2	21.89 ± 0.13	21.65 ± 0.03	0.24 ± 0.14	Y
d3	12:29:52.79	11:22:27.35	2.82	13.5	22.02 ± 0.14	21.73 ± 0.03	0.29 ± 0.15	N
d1 ··· d3	...	...	...	...	20.25 ± 0.06	19.90 ± 0.014	0.35 ± 0.06	...

Notes. Columns 4 and 5 give the distance from IC 3418. The last column indicates whether an Hα knot coincides with the object.

To estimate the restoring pressure on the gas disk, $P_{\rm rest} = 2\pi G\sigma_*\sigma_{\rm H}$, we first determine the stellar surface density, σ_*, from H-band observations. We next estimate the initial gas surface density, $\sigma_{\rm H}$, by assuming a pre-stripping H I mass and disk size based on IC 3418's morphology, optical luminosity, and optical radius. The H-band magnitude and effective surface brightness of IC 3418 are $m_{\rm H} = 12.72$ and $\mu_e = 22.24$ mag arcsec^{-2} (Gavazzi et al. 2000, 2003). Assuming a mass to light ratio of 0.78 (Kirby et al. 2008), $\sigma_* = 12\,M_\odot\,{\rm pc}^{-2}$ and $M_* = 10^{8.9}\,M_\odot$. Gavazzi et al. (2005) report an H I deficiency (see Giovanelli & Haynes 1983) and an upper limit on the H I mass that correspond to an expected $10^{8.8}\,M_\odot$ of H I in IC 3418. We estimate that IC 3418 contained 70% of its H I within 1.′85 by converting its UGC optical radius to a Holmberg radius (Dickel & Rood 1978) and taking an average ratio of the H I to optical disk size from Giovanelli & Haynes (1983). This gives $\sigma_{\rm H} \approx 2\,M_\odot\,{\rm pc}^{-2}$ and $P_{\rm rest} \approx 6\,M_\odot\,{\rm pc}^{-3}\,{\rm km}^2\,{\rm s}^{-2}$. A large initial gas fraction is consistent with IC 3418's blue optical-H color and low surface brightness.

We also considered the contribution of a Navarro–Frenk–White (NFW) dark matter halo to $P_{\rm rest}$; $P_{\rm rest,\,DM} = \sigma_{\rm H}\,(\partial\phi_{\rm NFW}/\partial r)$. We found that the dark halo makes a significant contribution to the restoring pressure, but that $P_{\rm ram} > P_{\rm rest}$ unless the halo mass exceeds $\approx 10^{13}\,M_\odot$. This is unrealistically high, and IC 3418's H I disk was extremely susceptible to RPS.

For the case of molecular cloud RPS, we assume spherically symmetric clouds with conservative values for a molecular cloud size and density of $r_{\rm MC} = 50$ pc and $\rho_{\rm MC} = 10^3$ cm^{-3}. This gives a surface density, $\sigma_{\rm H_2} = (4/3)\rho_{\rm MC} r_{\rm MC}$, of $\approx 2000\,M_\odot\,{\rm pc}^{-2}$. The restoring force from the stellar disk is $P_{\rm rest} = 2\pi G\sigma_*\sigma_{\rm H_2} \approx 6000\,M_\odot\,{\rm pc}^{-3}\,{\rm km}^2\,{\rm s}^{-2}$. For molecular clouds, $P_{\rm rest} \gg P_{\rm ram}$.

If IC 3418 is on a purely radial orbit and on its first pass through the cluster potential, then its tidal radius can be estimated by setting

$$\frac{\partial}{\partial r}\frac{Gm_{\rm IC\,3418}(r_t)}{r_t} = -r_t\frac{\partial}{\partial r}\frac{GM_{\rm Virgo}(r_o)}{r_o^2} \qquad (2)$$

and assuming NFW potentials. Here $m(r)$ denotes the mass enclosed within r, r_t the galaxy's tidal radius, and r_o the orbital radius within Virgo. This gives an upper limit on r_t; a more circular orbit will have a smaller tidal radius at IC 3418's current position. A lower limit can be estimated by using

$$\frac{m_{\rm IC\,3418}(r_t)}{m_{\rm IC\,3418}} = 0.58\left(\frac{r_o}{r_{v,\,\rm Virgo}}\right)^{0.50} \qquad (3)$$

(Mamon 2000), which assumes that the galaxy is at pericenter and that it has an orbital eccentricity typical of subhalos in N-body simulations. Here $r_{v,\rm Virgo}$ is Virgo's virial radius. For both estimates, we assume a dark matter to baryon mass ratio of $M_{\rm DM}/M_{\rm bary} \approx 15$ ($M_{\rm DM} \approx 10^{10.3}\,M_\odot$). We adopt $r_{v,\rm Virgo}$ from McLaughlin (1999).

IC 3418's current tidal radius is between 9 and 30 kpc. If the galaxy is not at pericenter, then its final tidal radius will be within 9 kpc. For comparison, its H-band effective radius is 4.6 kpc. While it is unlikely that IC 3418's disk is being tidally stripped, the tail may be tidally stripped from the galaxy as it passes through Virgo's core, thereby contributing to the ICL.

5. MORPHOLGY

Tails and arcs of young stars and/or H II regions which are consistent with an RPS origin have been observed in several clusters. C07 discovered two tails of young stars in deep *Hubble Space Telescope* imaging. One, an ∼0.1 L^* galaxy well within Abell 1689's X-ray halo, should be completely RP stripped, which is consistent with the declining SFR in the galaxy's disk observed by C07. The other, an L^* galaxy in Abell 2667, should be partially stripped (C07). Its asymmetric appearance and nuclear burst of star formation match simulations of partially RP stripped disks (Schulz & Struck 2001; Kronberger et al. 2008). Using Equation (3) and the same choice of parameters as C07, we estimate tidal radii beyond the stellar disk for both galaxies. Yoshida et al. (2008, Y08) discovered a tail of star-forming knots and young stellar filaments behind RB 199 in deep B, R_C, and Hα observations of the Coma cluster. Y08 estimate that the stellar disk is not tidally stripped, but that the gas disk is partially RP stripped. The galaxy ESO 137-001 in Abell 3627, a very dynamically young nearby cluster, was discovered to have an extended X-ray tail in which multiple H II regions were detected (Sun et al. 2006, 2007).

Galaxies with arcs of H II regions following the bow shock morphology of the H I have been observed in Virgo (Kenney

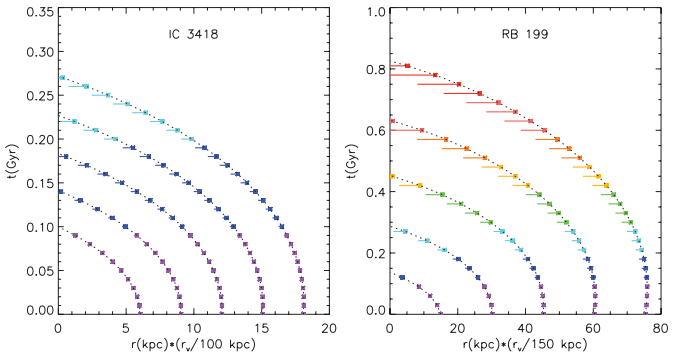

Figure 4. Simple model of tail morphology for tails resembling IC 3418 (left) and RB 199 (right). Tracks represent a filament falling back onto the galaxy. Line segments show the diverging orbits of two episodes of star formation separated by $t_{\rm form} = 100$ Myr. The divergence of the orbits is due to an additional $a_{\rm MC}$ which is applied to the later forming stars for the first $t_{\rm form}$. The segments change color every 100 Myr.

& Koopmann 1999) and Abell 1367 (Gavazzi et al. 2001). The morphology of these arcs suggests cloud stripping, but cloud formation likely occurred in the shock compressed gas while clouds in the outer disk were dissociated and then stripped. Isolated dense clouds can be ablated by the ICM wind (Nulsen 1982; Raga et al. 1998), dissociated if a shock is driven directly into them (Aannestad 1973), and heated by star formation and then stripped (Kenney et al. 2004).

We advance a basic mechanism to account for the tails' morphologies, which are characterized by isolated knots, long filaments, and intermediate "streamers" such as that in IC 3418 (d1/k1). Giant molecular clouds may spawn multiple episodes of star formation. The cloud experiences a force from the ICM wind, but the newly formed stars do not. Due to the differing accelerations, the newly formed stars are essentially dropped from the cloud, which itself is supported by the ICM wind. The cloud trails a filament of stars.

The details of the tails' morphologies provide a probe of their formation. To first order, a cloud forms a filament of length $(1/2)a_{\rm MC}\Delta t_{\rm form}^2$, where $a_{\rm MC}$ is the acceleration due to the ICM wind, $a_{\rm ICM}$, on the molecular cloud and $\Delta t_{\rm form}$ is the time between the cloud's first and last episodes of star formation. In the cloud's frame, the stars accelerate toward the galaxy with $a_{\rm MC}$. Large $a_{\rm MC}$ create long filaments. Accordingly, the long stellar filaments behind RB 199 are indicative of large $a_{\rm MC}$, itself characteristic of dynamical coupling between the gas phases and therefore of cloud stripping. The $a_{\rm ICM}$ can be estimated as $P_{\rm ram}/\sigma_{\rm gas}$, or, for the H I disk,

$$a_{\rm H} = 0.02\,{\rm kpc\,Myr^{-2}} \left(\frac{P_{\rm ram}}{40\,M_\odot\,{\rm pc^{-3}\,km^2\,s^{-2}}}\right)\left(\frac{2\,M_\odot\,{\rm pc^{-2}}}{\sigma_{\rm H}}\right),$$

which can form a 10 kpc filament in 30 Myr. Assuming molecular clouds that are not dynamically coupled to the H I, $a_{\rm H_2}/a_{\rm H} = \sigma_{\rm H_2}/\sigma_{\rm H} \approx 10^{-3}$ (see Section 4), corresponding to much shorter "filaments."

The treatment above assumes that the cloud and its filament orbit together. In contrast, both tides, which increase the distance between two episodes as they fall, and the ICM wind, which continuously increases the orbital energy of a cloud while it exists, work to lengthen filaments. Therefore, if $a_{\rm MC} = a_{\rm H}$, then *only* long filaments are formed, which conflicts with the observations. We show below that a plethora of morphologies can be formed with $a_{\rm MC} = a_{\rm H_2}$.

The influences of both gas physics and gravity are observed, requiring us to consider both forces. The streamer in IC 3418's tail and the filaments observed by Y08 and C07 are located close to the galaxy, where tidal forces are strongest. The extended objects are also redder, indicating that they are older and therefore potentially more dynamically evolved. On the other hand, the streamer in IC 3418 shows a strong UV color gradient and, in RB 199, when a star-forming knot is associated with a filament, it is found downwind. Both highlight the role of the ICM wind.

Figure 4 illustrates the next step in modeling complexity. We postulate clouds that are generated with a moderate initial velocity heading away from the galaxy. These clouds fall back toward the galaxy. Each track with its related line segments represents two episodes of star formation separated by $t_{\rm form} = 100$ Myr, which is motivated by the UV gradient in the streamer, as they fall in an NFW potential. Both episodes have the same initial orbit, but the higher, later forming, episode has an additional acceleration for the first $t_{\rm form}$. The line segments represent potential knots and filaments.

In simulations, RP stripped gas is accelerated to the rest velocity of the ICM, but travels away from the galaxy as it accelerates. Gas located close to the galaxy has a lower velocity with respect to the galaxy and turbulent flow around the disk can cause gas to actually fall back onto the galaxy from the wake (Roediger & Brüggen 2008, R08). In the model, increasing a cloud's initial velocity increases the filament length until the velocity exceeds the escape velocity and the knot speeds away without forming a filament.

The left and right panels of Figure 4 represent the tails of IC 3418 and RB 199, respectively. They are differentiated by their overall length scale and age. In each, $P_{\rm ram}$ is within the range allowed by observations. In simulations, tail length is determined by the mass loss per orbital length, which will vary considerably between galaxies (R08).

Several suggestive features are reproduced in Figure 4. Knots, short streamers, and long filaments all form. As seen in the observations, the filaments' lengths and ages are correlated, particularly for neighboring objects, and in each tail the longest filaments are found closest to the galaxy. For a nice example of the first feature, compare d2 and its surrounding knots. That a simple variation in the length scale reproduces both IC 3418 and RB 199 is an additional success. Tail morphologies are rich with information about their formation mechanisms, which should motivate further modeling. The current work indicates that the observations favor in situ cloud formation or at least $a_{\rm MC} = a_{\rm H_2}$.

6. DISCUSSION

RPS of H I is the only theoretically favored means of removing mass from IC 3418's disk at its current position in the Virgo Cluster. Nevertheless, star formation is occurring in the galaxy's wake, requiring the presence of H_2. We suggest that H_2 forms within the stripped wake aided by turbulence. Turbulence in the wakes of RP stripped galaxies has been seen in both simulations (R08) and observations (Yoshida et al. 2004). In simulations, turbulence can drive both the formation of star clusters within clouds (Padoan & Nordlund 2002) and cloud formation itself (Mac Low & Klessen 2004). The quasi-scale free hierarchical nature of turbulence works to enhance density contrasts in a turbulent region, increasing the chance that gas can cool and collapse. An alternate theory requires that the H_2 in the disk is tightly dynamically bound to the H I, though no mechanism for

this binding is advanced. We have shown that the morphologies of the tails disfavor this interpretation.

Further constraining the tails' formation mechanism, and in particular the possible role of turbulence, will require additional observations and improved modeling, presumably using hydrodynamical simulations. Deep, high-resolution, imaging of one or more tails in multiple optical bands, UV, and Hα, for which IC 3418 is a prime candidate, could provide detailed constraints on a model of tail formation.

IC 3418's tail represents a novel environment in which to study cloud and star formation. The SFR within the normal star-forming disk of a massive galaxy correlates with the gas surface density (Toomre 1964; Kennicutt 1989, 1998; Martin & Kennicutt 2001). In other environments, the SFR does not follow a Schmidt–Kennicutt Law. Examples are extended gas disks (Ferguson et al. 1998; Thilker et al. 2007; Bigiel et al. 2008), low surface brightness disks (Wyder et al. 2009), and dwarf irregular galaxies (Hunter & Elmegreen 2006; Lee et al. 2009). Gravitational effects, turbulence, magnetic fields, and thermal support may all play a role in cloud and star formation. Determining the role that each plays in driving and regulating star formation will require studying multiple regimes.

This research has made use of the GOLD Mine Database and of the NASA/IPAC Extragalactic Database (NED) which is operated by the Jet Propulsion Laboratory, California Institute of Technology, under contract with the National Aeronautics and Space Administration. The authors thank L. Cortese for helpful comments.

REFERENCES

Aannestad, P. A. 1973, ApJS, 25, 223
Bigiel, F., Leroy, A., Walter, F., Brinks, E., de Block, W. J. G., Madore, B., & Thornley, M. D. 2008, AJ, 136, 2846
Binggeli, B., Tammann, G. A., & Sandage, A. 1987, AJ, 94, 251
Chung, A., van Gorkom, J. H., Kenney, J. D. P., Crowl, H., & Vollmer, B. 2009, AJ, 138, 1741
Chung, A., van Gorkom, J. H., Kenney, J. D. P., & Vollmer, B. 2007, ApJ, 659, 115
Cortese, L., et al. 2007, MNRAS, 376, 157
Crowl, H., Kenney, J. D. P., van Gorkom, J. H., & Vollmer, B. 2005, AJ, 130, 65
Dickel, J. R., & Rood, H. J. 1978, AJ, 223, 391
Ferguson, A. M. N., Wyse, R. F. G., Gallagher, J. S., & Hunter, D. A. 1998, ApJ, 506, 19
Gavazzi, G., Boselli, A., Cortese, L., Arosio, I., Gallazzi, A., Pedotti, P., & Carrasco, L. 2006, A&A, 446, 839
Gavazzi, G., Boselli, A., Donati, A., Franzetti, P., & Scodeggio, M. 2003, A&A, 400, 451
Gavazzi, G., Boselli, A., Mayer, L., Iglesias-Paramo, J., Vílchez, J. M., & Carrasco, L. 2001, ApJ, 563, 23
Gavazzi, G., Boselli, A., van Driel, W., & O'Neil, K. 2005, A&A, 429, 439
Gavazzi, G., Franzetti, P., Scodeggio, M., Boselli, A., & Pierini, D. 2000, A&A, 361, 863
Gavazzi, G., Zaccardo, A., Sanvito, G., Boselli, A., & Bonfanti, C. 2004, A&A, 417, 499
Giovanelli, R., & Haynes, M. P. 1983, AJ, 88, 881G
Gunn, J. E., & Gott, J. R. 1972, ApJ, 176, 1
Hunter, D. A., & Elmegreen, B. G. 2006, ApJS, 162, 49
Kapferer, W., Sluka, C., Schindler, S., Ferrari, C., & Ziegler, B. 2009, A&A, 499, 87
Kenney, J. D. P., & Koopmann, R. A. 1999, AJ, 117, 181
Kenney, J. D. P., van Gorkom, J. H., & Vollmer, B. 2004, AJ, 127, 3361
Kennicutt, R. C. 1989, ApJ, 344, 685
Kennicutt, R. C. 1998, ApJ, 498, 541
Kirby, E. M., Jerjen, H., Ryder, S., & Driver, S. P. 2008, AJ, 136, 1866
Kronberger, T., Wapferer, W., Ferrari, C., Unterguggenberger, S., & Schindler, S. 2008, A&A, 481, 337
Lee, J., et al. 2009, ApJ, 706, 599
Mac Low, M.-M., & Kelssen, R. S. 2004, Rev. Mod. Phys., 76, 125
Mamon, G. A. 2000, in ASP Conf. Ser. 197, Dynamics of Galaxies: from the Early Universe to the Present, ed. F. Combes, G. A. Mamon, & V. Charmandaris (San Francisco, CA: ASP), 377
Martin, C. L., & Kennicutt, R. C. 2001, ApJ, 555, 301
Martin, C., et al. 2005, ApJ, 619, L1
McLaughlin, D. E. 1999, ApJ, 512, 9
Mei, S., et al. 2007, ApJ, 655, 144
Nulsen, P. E. J. 1982, MNRAS, 198, 1007
Padoan, P., & Nordlund, Å. 2002, ApJ, 576, 870
Raga, A. C., Cantó, J., Curiel, S., & Taylor, S. 1998, MNRAS, 295, 738
Roediger, E., & Brüggen, M. 2008, MNRAS, 388, 465
Salim, S., et al. 2007, ApJS, 173, 267
Sanderson, A. J. R., Ponman, T. J., Finoguenov, A., Lloyd-Davies, E. J., & Markevitch, M. 2003, MNRAS, 340, 989
Schindler, S., Binggeli, B., & Böhringer, H. 1999, A&A, 343, 420
Schulz, S., & Struck, C. 2001, MNRAS, 328, 185
Sun, M., Donahue, M., & Voit, G. M. 2007, ApJ, 671, 190
Sun, M., Jones, C., Forman, W., Nulsen, P. E. J., Donahue, M., & Voit, G. M. 2006, ApJ, 637, 81
Thilker, D. A., et al. 2007, ApJS, 173, 538
Tonnesen, S., & Bryan, G. L. 2009, ApJ, 694, 789
Toomre, A. 1964, ApJ, 139, 121
Wyder, T. K., et al. 2009, ApJ, 696, 1834
York, D. G., et al. 2000, AJ, 120, 1579
Yoshida, M., et al. 2004, AJ, 127, 90
Yoshida, M., et al. 2008, ApJ, 688, 918